Available online at www.sciencedirect.com
SCIENCE DIRECT®
Peptides 26 (2005) 1697–1711
PEPTIDES
www.elsevier.com/locate/peptides

Dose–response effects of ectopic agouti protein on iron overload and age-associated aspects of the A^{vy}/a obese mouse phenome

George L. Wolff [a,*], Paul Whittaker [b]

[a] *Division of Biochemical Toxicology, National Center for Toxicological Research, Food and Drug Administration, Jefferson, AR 72079-9502, USA*
[b] *Center for Food Safety and Applied Nutrition, Food and Drug Administration, College Park, MD 20740-3835, USA*

Received 14 July 2004; accepted 16 December 2004
Available online 27 June 2005

Abstract

Isogenic and congenic offspring from matings of inbred black *a*/*a* dams by sibling (or non-sibling from another inbred strain) yellow agouti A^{vy}/a sires provide an animal model of obese yellow agouti A^{vy}/a and isogenic lean pseudoagouti A^{vy}/a mice exhibiting two different in vivo concentrations (high, very low) of ectopic agouti protein (ASP) with congenic lean black *a*/*a* mice as null controls. This makes it possible to differentiate between the high and very low dose levels of ectopic ASP with respect to interactions with diverse physiological and molecular pathways. Assay of differential responses to 12 or 24 months of carbonyl iron overload assessed the possible suitability of this animal model for the study of hemochromatosis. Agouti *A*/*a* B6C3F$_1$ mice were used as non-congenic null controls. The age-related waxing and waning of body weight, food consumption, and caloric efficiency, as well as associated changes in pancreatic islets and islet cells, and formation of liver tumors were assayed. While the hypothesis that these mice might serve as a tool for investigating hemochromatosis was not confirmed, the data did provide evidence that even the very low levels of ASP in pseudoagouti A^{vy}/a mice affect the network of molecular/metabolic/physiological response pathways that comprises the yellow agouti obese phenome. We suggest that the combination of yellow agouti A^{vy}/a, pseudoagouti A^{vy}/a, and black *a*/*a* congenic mice provides a practical tool for applying a dose–response systems biology approach to understanding the dysregulatory influence of ectopic ASP on the molecular-physiological matrix of the organism.
Published by Elsevier Inc.

Keywords: Agouti protein; Caloric efficiency; Hepatocellular tumors; Hyperplasia; Iron overload; Melanocortin receptor 4; Obesity; Pancreatic islet cells; Pseudoagouti mice; Systems biology; Age-associated weight loss

1. Introduction

Iron overload is a condition associated with hereditary or secondary disturbance of iron metabolism. Hereditary hemochromatosis is a disorder with an autosomal recessive pattern of inheritance and is the most common genetic disease among Northern European populations, affecting 1 in 400 individuals and has an estimated carrier frequency of 1 in 10 [7]. Hemochromatosis is characterized by enhanced gastrointestinal absorption of iron that leads to a progressive increase of iron stores throughout life [38]. The increased intestinal absorption of iron in hemochromatosis results in deposition of iron in parenchymal organs, eventually leading to cirrhosis, hepatocellular carcinoma, diabetes mellitus, and congestive heart failure.

A possible mechanism for damage from chronic iron overload may be the effect of free radical formation and lipid peroxidation. Whittaker et al. [39] previously reported that liver lipid peroxides were significantly increased in iron-overloaded rats. Lipid peroxidation is a chain reaction that is increased by iron and may have pathophysiologic consequences in diseases.

The age-associated involvement of the pancreas and occurrence of diabetes mellitus in yellow agouti A^{vy}/a mice plus their increased susceptibility to formation of hepatocellular adenoma and carcinoma [46,47] suggested that they might be suitable as an animal model for the study

* Corresponding author. Tel.: +1 501 225 5964; fax: +1 501 225 5863.
E-mail address: gwolffar@prodigy.net (G.L. Wolff).

0196-9781/$ – see front matter. Published by Elsevier Inc.
doi:10.1016/j.peptides.2004.12.033

of hemochromatosis. Subsequent to a 90 day dose-finding study [36], a chronic (2 years) study of iron overload was conducted using three male mouse phenotypes segregating among C57BL/6N × YS F_1 hybrid offspring that exhibit, respectively, high, very low, and absent levels of ectopic agouti protein (ASP); namely, obese viable yellow agouti A^{vy}/a, lean pseudoagouti A^{vy}/a, and lean black a/a. This hypothesis was not confirmed by the data generated in this chronic study; however, the study did provide information on the interaction effects of different levels of ectopic ASP and iron overload on several aspects of mouse physiology.

A unique feature of this experimental design was that the in vivo effects of low levels of ectopic ASP could be ascertained by comparing any physiological or metabolic parameter from the lean pseudoagouti mice with that from the congenic lean black mice. Black a/a mice produce pheomelanin only in hair follicles in the ear and perineal areas [11] and not in ectopic sites. Additionally, the differential responses to iron overload of yellow agouti A^{vy}/a mice, compared with the other mouse phenotypes, emphasize that mutations alter the physiological/metabolic response patterns of the organism by altering the relations among molecular processes and pathways.

Obesity is the visible sign of serious dysregulations in the homeostatic network of metabolic and physiologic pathways that regulate energy metabolism and the intake and utilization of nutrients. However, obesity is not an all-or-none phenomenon but is merely "an easily detected and quantifiable phenotypic endpoint" of patterns of metabolic dysregulations that may be unique to each individual [50]. Therefore, "obesity" does not define a specific disease state but only a symptom common to dysregulation of different homeostatic pathways. Basically, an organism that utilizes fewer calories than it ingests, stores the excess calories as fat in adipose tissue.

Here we delineate age-associated physiologic and molecular variability inherent in a specific "obesity phenome" induced by the continous ectopic transcription of the *agouti* gene on chromosome 2 of *Mus musculus*. Normally, the agouti signaling protein specified by this gene determines only the synthesis of yellow pigment (pheomelanin) in the melanocytes of hair follicles.

This obesity phenome differs in numerous physiologically important characteristics from other obesity phenomes, e.g., that exhibited by Le^{ob}/Le^{ob} mice [50]. Indeed, the deposition of excessive fat stores per se is merely one of a number of end results induced by the dysregulation of diverse metabolic and molecular signaling pathways by different mutant proteins.

The complexity of the yellow agouti obese mouse phenome (syndrome) is attributable to the nature of the mutation. Whereas transcription of the species-type A^w and A alleles at the *agouti* locus is temporally and spatially restricted, transcriptional regulation of the yellow agouti mutant alleles is not so restricted. During formation of the hair in $A^w/-$ and $A/-$ mice, α-melanocyte stimulating hormone (α-MSH) binds to melanocortin 1-receptors (MC1R) [25] on hair bulb melanocytes, inducing synthesis of black pigment (eumelanin). This is followed by a brief period during which transcription of the *agouti* gene occurs in the hair follicle cells producing ASP that binds to MC1R, thereby preventing binding of α-MSH. Failure of MC1R to bind α-MSH results in synthesis of the default pigment pheomelanin, rather than eumelanin, that is deposited in the growing hair. After a period of several days, ASP synthesis ceases and eumelanin synthesis resumes. This chain of events produces a yellow subapical band, characteristic of the agouti pattern, on an otherwise eumelanic hair but has no obvious effect on body weight.

In viable yellow agouti $A^{vy}/-$ mice, on the other hand, ASP is continuously synthesized in essentially all tissues [6]. This is due to insertion of an intracisternal A particle (IAP) into exon 1A of the *agouti* gene, resulting in the usurpation of transcriptional regulation of *agouti* by a constitutively active cryptic promoter in the 5′ long terminal repeat (LTR) of the IAP [3,23]. Continously synthesized ectopic ASP, present in tissues other than hair follicles, interacts with diverse gene products and molecular/metabolic pathways to transform a normal mouse into one characterized by the "yellow agouti obese mouse phenome."

Responsiveness to iron overload and induction of liver enzymes by promoters of hepatotumorigenesis, such as phenobarbital [48] are also altered by this change in transcriptional regulation of the *agouti* gene. Temporal changes in hormonal patterns, such as those of IGF-I, for example (reviewed in [53]), are also induced.

Differences in the carcass lipogenesis rates between yellow agouti A^{vy}/a and black a/a mice at younger and older ages reflect the development of obesity in the yellow agouti mice [55]. In mice aged 2 ± 0.5 months, A^{vy}/a mice had a 24% higher rate of ^3H_2O incorporation/g carcass weight than a/a mice. By age 5–8 months the incorporation rate was 44% higher in the A^{vy}/a mice. This difference can be accounted for by decreased incorporation rates with age so that there is a 22% decrease in black mice, but only a 9% decrease in yellow mice. As a consequence, at the younger age the A^{vy}/a mice contained 94% more body fat than the a/a mice, whereas in the older mice the difference had increased to 349% (reviewed in [50]).

While yellow agouti mice tend to eat somewhat more food than non-yellow mice [8], a major part of their greater adiposity results from more efficient calorie utilization which, however, is abolished by 30% caloric restriction [52]. This greater efficiency is graphically illustrated by the amount of feed consumed per gram body weight gain between 16 and 44 weeks of age:

	Ad Lib (g)	Calorie restricted (g)
A^{vy}/A	8.7	30.5
A/a	28.4	28.0

Between 12 and 51 weeks of age ad lib-fed A^{vy}/a mice gained 128% in body weight compared with only 41% for comparable A/a mice. Calorically restricted A^{vy}/a and A/a mice, on the other hand, gained only 16% and 21%, respectively.

A primary determinant of nutrient intake, efficiency of calorie utilization, energy metabolism and body weight in mice is melanocortin 4-receptor (MC4R) signaling in the hypothalamus. Its normal antagonist is agouti-related protein (AGRP) [1]; however, in yellow agouti mutants, constitutively synthesized ectopic ASP assumes the role of primary MC4R antagonist resulting in disruption of MC4R signaling. This, in turn, induces development of obesity in non-yellow mice [16], suggesting that several aspects of this syndrome, e.g., increased food consumption, obesity, and increased body size, are mediated by the inhibition of signaling by MC4R on hypothalamic neurons by ectopic ASP.

Not all viable yellow agouti A^{vy}/a mice become obese; a small proportion remains in the body weight range of non-mutant mice (Table 10). Furthermore, the body weights of the A^{vy}/a mice that did become obese varied over a considerable range. In old age these mice gradually lost weight so that by 2 years, their weight had become "normal." The relative roles, if any, of ASP and MC4R signaling in these variations in body weights are unknown.

The very similar lean "pseudoagouti" A^{iapy}/a [22] and A^{vy}/a [51] phenotypes both result from cessation of continous ectopic *agouti* gene transcription due to methylation of CpG islands in the LTR of the inserted IAP. Transcription occurs only in the skin and hair follicles during formation of the subapical yellow band, resulting in a pattern grossly resembling the species-type agouti pattern [10]. The increased carcass weight of pseudoagouti A^{vy}/a mice compared to their congenic black *a*/*a* littermates [47], and the presence of very low levels of ASP in all tissues of pseudoagouti A^{vy}/a mice [6] suggest the existence of clones of cells [24] in which methylation of the IAP promoter has not occurred, e.g., in the yellow areas of the coat, so that ectopic ASP is synthesized, albeit at very low levels (reviewed in [51]).

The present data delineate altered phenomic characteristics associated with chronic iron overload and ageing from 12 to 24 months of age, such as body weight, feed consumption, metabolic efficiency, histopathology of pancreas, heart, and liver, numbers of pancreatic α, β, and δ cells/mean islet area, pancreatic islet numbers and areas, and hepatocellular tumors in two phenotypes of $C5YSF_1$ hybrid A^{vy}/a male mice, namely obese yellow agouti and lean pseudoagouti, their congenic black *a*/*a* littermates, and non-congenic $B6C3F_1$ hybrid mice.

2. Materials and methods

2.1. Animals and housing conditions

To increase the likelihood of detecting effects of Fe overload on hepatocellular tumor formation two inbred strains with known low spontaneous prevalences of such tumors were chosen to produce the F_1 hybrid offspring used for the study. Standard $B6C3F_1$ mice were used as non-congenic controls for strain background.

Weanling male F_1 hybrid mice from the following crosses were produced in the NCTR breeding colony:

C57BL/6NNctr × YS/WffC3Hf/Nctr-A^{vy} → $C5YSF_1$-yellow (A^{vy}/a) + $C5YSF_1$-pseudoagouti (A^{vy}/a) + $C5YSF_1$-black (a/a);
C57BL/6NNctr × C3H-MTV$^-$/Nctr → $B6C3F_1$.

Twelve male mice, about 5 weeks old, of each F_1 hybrid genotype/phenotype were assigned to each of four dose groups (35, 1500, 3500 μg/g, 5000 μg carbonyl iron/g AIN-93M diet) to be sacrificed after 12 months on dose and were maintained in covered polycarbonate cages.

Forty-eight male mice (4/cage) of each F_1 hybrid genotype/phenotype, to be sacrificed after 24 months on dose, were allocated over 3–4 weeks to each of the four dose groups (35, 1500, 3500 μg/g, 5000 μg carbonyl Fe/g AIN-93M diet). Due to an insufficient number of pseudoagouti A^{vy}/a mice available, the 5000 μg carbonyl Fe/g diet group was omitted for this phenotype; thus, 3500 μg Fe/g diet was its highest dose group.

All mice were maintained four per covered polycarbonate cage with sterilized hardwood chips (P.J. Murphy Forest Products Corp., Rochelle Park, NJ) as bedding. AIN-93M diets, containing various levels of carbonyl Fe (see above), were fed ad libitum. Millipore-filtered water was always available. Cages and water bottles were changed weekly. Room temperature was maintained at 22 ± 2 °C and relative humidity at 50 ± 5% with 15–17 changes of air/h. Fluorescent light cycles of 12 h on (6 a.m.–6 p.m.) and 12 h off (6 p.m.–6 a.m.) were automatically regulated.

This study was approved by the NCTR Institutional Animal Care and Use Committee prior to implementation.

2.2. Diets

Carbonyl Fe (35, 1500, 3500, or 5000 mg) (ISP Technologies Inc., Wayne, NJ) was incorporated into each kg AIN-93M diet (Dyets Inc., Bethlehem, PA). The AIN-93M diet included (g/kg) casein 140.0, L-cystine 1.8, cornstarch 464.457 (control) to 459.492 (highest Fe), DYETROSE 155.0, Dextrose 100.0, Solka-Floc cellulose 50.0, soybean oil 40.0, choline bitartrate 2.5, *t*-butylhydroquinone 0.008, Cu/dextrose pre-mix (5 mg/g) 1.2, AIN-93M salt mix (w/o Fe) 35.0, AIN-93M vitamin mix 10.0 [29]. It should be noted that, in the previous dose-finding study for iron overload [40], the AIN-76A diet was used.

2.3. Histopathology assays

At the end of the 12 or 24 months feeding periods, the mice were fasted for approximately 15 h. A complete necropsy was performed on each animal and tissues were fixed in 10% neutral-buffered formalin. Tissue specimens were then trimmed, processed through an ascending ethanol series and xylene, embedded in paraffin and sectioned at 5 μm. One set of tissues was stained with hematoxylin and eosin.

Another tissue set of the pancreas, liver, and heart was reacted with Perl's Prussian blue for Fe. This involves colorless potassium ferricyanide reacting with ferric ions to create an insoluble blue ferric ferrocyanide [20,36].

2.4. Pancreas morphometry

To ensure uniform diameter of sections of equivalent area, pancreatic tissues were adhered to filter paper and fixed in 10% neutral-buffered formalin. Procedures for embedding, sectioning, staining, and evaluating the pancreas were standardized to assure uniformity. Five micrometers of serial sections were cut from each paraffin embedded pancreas and mounted on positively charged slides. All tissue sections were immunostained using the StreptAvidin peroxidase detection system with DAB (3,3′-diaminobenzidine) as the chromogen substrate and Mayer's hematoxylin as the counterstain.

For labeling of the α cells one section from each pancreas was incubated with a polyclonal antibody to Glucagon (Dako Corp.), 1:600 dilution; for labeling of the β cells a second adjacent section was incubated with a polyclonal antibody to Insulin (Dako Corp.), 1:600 dilution; and for labeling of the δ cells a third adjacent section was incubated with a polyclonal antibody to Somatostatin (Dako Corp.), 1:800 dilution. Cells were counted and areas measured using the Optimas Image Analysis System (Optimas Corp., Edmonds, WA). All islets present in the representative sections of each pancreas were evaluated for α, β, and δ cell number and islet areas.

2.5. Data analysis

2.5.1. Body weight and food consumption

Individual body weights and cage food consumption were collapsed into weekly time intervals. Every fourth week from week 6 to week 110 was used for the analyses. A heterogeneous autoregressive model for the covariance structure of repeated measurements on the same cage was used. This model assumes that the correlation of measurements on the same subject depends on the time between measurements. The correlation is assumed to decrease exponentially with the time between measurements. A different covariance is estimated for each time period in the analyses in this "heterogeneous" model.

There was a two-way fixed effect treatment structure with dose and strain as the treatments. Repeated measurements in time were also considered. Independent *t*-tests on dose were done by phenotype/strain and week. Holm's adjusted independent *t*-tests [15] on strain were done by dose and week. These tests make possible pairwise comparisons of the different phenotypes and make an adjustment for the fact that several comparisons per dose group and week are carried out concurrently. Alpha = 0.05 was used as the significance level.

2.5.2. Pancreatic islets

The mean islet area and number of islets were analyzed separately. An initial three-way analysis of variance (ANOVA) was conducted, in which all three factors – dose, time, and tumor – were crossed with one another. The SAS procedure MIXED was used and effects of all orders were tested.

The results showed the tumor main effect and all interaction effects with tumor were not significant at the 5% level; therefore, the tumor effect was not included in the final model.

In the final model, a two-way ANOVA with two main effects – dose and time – and their interaction was refitted and used for statistical testing. The procedure of Holm [15] was used to adjust for multiple comparisons for each end point. Significance was assumed at alpha less than the 0.05 level.

2.5.3. Pancreatic islet cells

Independent *t*-tests were done to test for differences, by phenotype and dose, in the average number of α, β, or δ cells per mean islet area between 12 and 24 months. The Shapiro–Wilk's normality test [32] was used to verify that the data were normally distributed. Next, the Folded *F* statistic [35] tested for equal variances between groups. If this statistic was significant, the Satterthwaite approximation [31] was used to compute the *t* statistic. Otherwise, the pooled variance was used in the computations.

To ascertain if differences between 12 and 24 months were similar for both control (35 μg/g Fe) and high (3500 μg/g Fe for pseudoagouti, 5000 μg/g Fe for the other phenotypes) dose groups, a second *t*-test, using the same steps as above, was done by phenotype and number of α, β, or δ cells per mean islet area.

3. Results

3.1. Body weight and food consumption

Body weight of yellow agouti A^{vy}/a mice peaked at week 66 and then decreased markedly till the end of the study at week 109 (Fig. 1).

Body weight of black *a*/*a* mice peaked at week 70 and gradually decreased slightly to week 109 (Fig. 1).

Body weight of $B6C3F_1$ mice increased at a greater rate than the black mice to week 18, peaked at week 66, then decreased very slightly to week 109 (Fig. 1).

Food consumption of yellow agouti mice was greater than that of black mice until about week 34. At this time there was a decrease in food consumption by all phenotypes which, in the case of the black mice, stabilized until week 94. Among the yellow agouti mice, however, the rate of food consumption rebounded till week 54 and then decreased continually until week 90 (Fig. 2).

Food consumption of $B6C3F_1$ mice started at a higher level than black mice, but lower than yellow agouti mice,

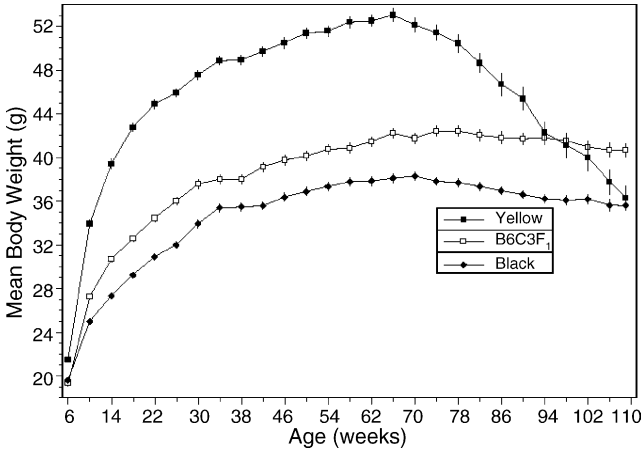

Fig. 1. Body weight curves of control yellow agouti A^{vy}/a, control + treated black a/a, and B6C3F$_1$ male mice.

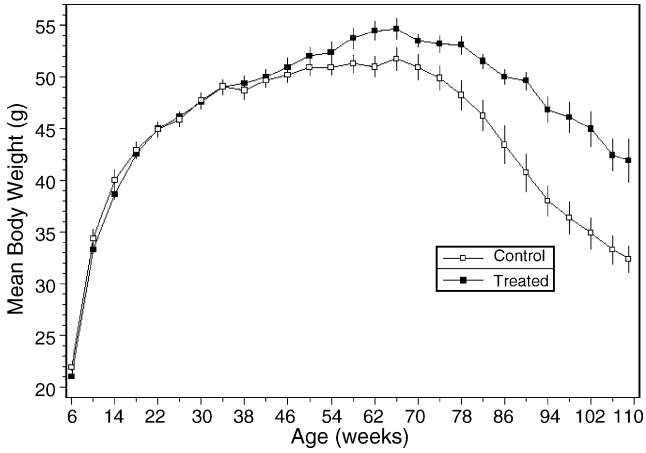

Fig. 3. Body weight curves of yellow agouti A^{vy}/a male mice fed 35 (control) or 5000 μg/g (treated) carbonyl Fe.

and increased to week 46. It then leveled off till week 70 at which time there was a decrease and stabilization at a new level till week 102 (Fig. 2).

3.1.1. Yellow agouti mice and Fe overload

A positive effect of Fe overload on body weight, i.e., decreased rate of weight loss, was observed only among the yellow agouti A^{vy}/a mice, beginning about week 58 ($P = 0.05$) and continuing through the end of the study at week 109 ($P < 0.001$) (Fig. 3). Resource limitations dictated that only the data from the 35 and 5000 μg/g [3500 μg/g for pseudoagouti] carbonyl Fe groups were analyzed statistically.

Food consumption of the treated mice remained relatively uniform throughout the study. Iron overload appeared to ameliorate, via unknown pathways, the rather drastic decrease in food consumption among the untreated yellow agouti A^{vy}/a between weeks 54 and 90. Between weeks 18 and 38, food consumption among the treated A^{vy}/a mice was lower ($P = 0.01$) than among the control A^{vy}/a mice. In contrast, between weeks 82 and 102 food consumption was higher ($P = 0.001$) among the treated than among the control groups (Fig. 4).

3.1.2. Pseudoagouti, black, and B6C3F$_1$ mice

Body weights and food consumption of the control and treated groups of each phenotype (black a/a, pseudoagouti A^{vy}/a, and B6C3F$_1$ A/a) mice were similar (data not shown). Therefore, Figs. 1, 2, 5–8 are based on the combined data from the control and treated mice in each of these phenotypes.

3.1.3. Food consumption: body weight ratio.

The mean ratio of food consumption: body weight of yellow agouti mice decreased continuously from week 6 to week 38, leveled off to week 54, and then stabilized at a lower level to week 90, at which point it rose rapidly to week 102 (Fig. 7). The relatively lower ratio of the yellow agouti mice presumably reflects the higher metabolic efficiency associated with the presence of ectopic ASP [52].

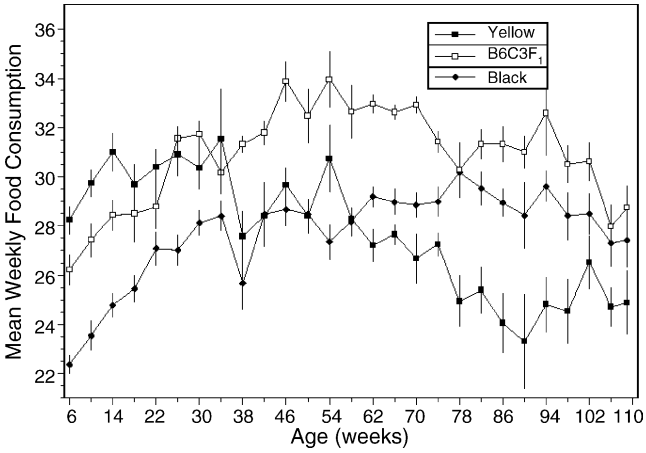

Fig. 2. Food consumption curves of control yellow agouti A^{vy}/a, control + treated black a/a, and B6C3F$_1$ male mice.

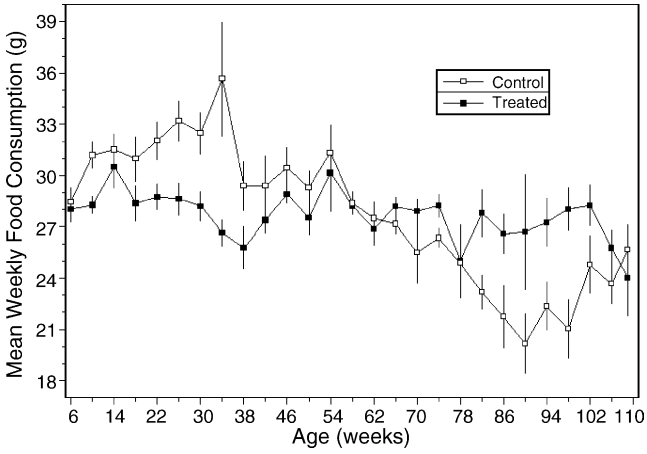

Fig. 4. Food consumption curves of yellow agouti A^{vy}/a male mice fed 35 (control) or 5000 μg/g (treated) carbonyl Fe.

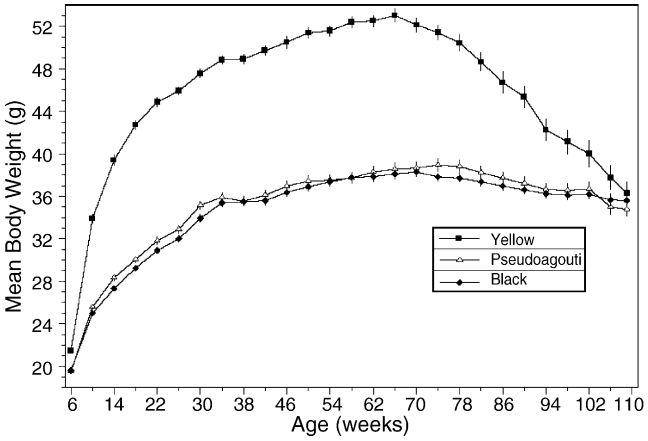

Fig. 5. Body weight curves of control yellow agouti A^{vy}/a, and control + treated pseudoagouti A^{vy}/a, and black a/a male mice.

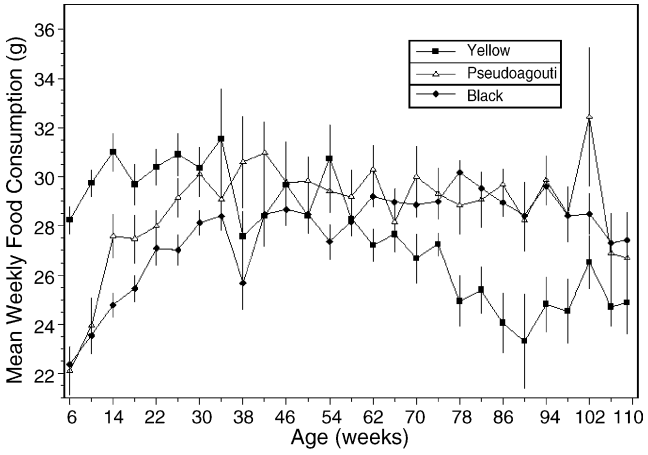

Fig. 6. Food consumption curves of control yellow agouti A^{vy}/a, and control + treated pseudoagouti A^{vy}/a, and black a/a male mice.

In contrast, the mean ratio among B6C3F$_1$ mice decreased between weeks 6 and 34, then stabilized to week 70, decreased to week 78 and remained at that level till week 102 (Fig. 7).

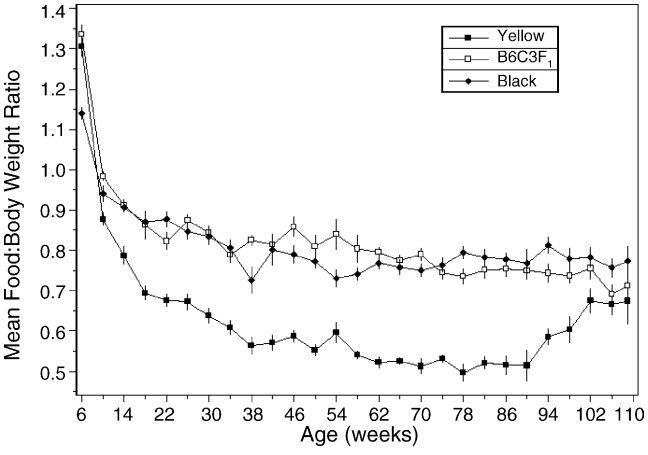

Fig. 7. Food consumption: body weight ratios of control yellow agouti A^{vy}/a, control + treated black a/a, and B6C3F$_1$ male mice.

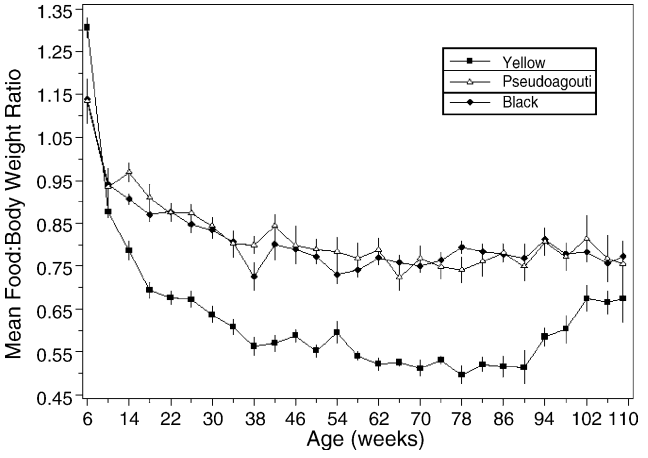

Fig. 8. Food consumption: body weight ratios of control yellow agouti A^{vy}/a, and control + treated pseudoagouti A^{vy}/a, and black a/a male mice.

The pattern of mean ratios among the pseudoagouti A^{vy}/a mice was similar to that observed among the black a/a and B6C3F$_1$ mice (Figs. 7 and 8).

3.2. Pancreas

3.2.1. Islets

Total islet area per pancreas increased with age in all mice (Table 1), whereas mean islet area per pancreas increased with age only among the black and B6C3F$_1$ mice (Table 2). The mean number of islets per pancreas also increased with age in all mouse phenotypes (Table 3).

Only among the yellow agouti mice did iron overload exert any significant effect. Namely, it significantly decreased the mean number of islets per pancreas, mean islet area, and mean total islet area at both 12 and 24 months of age (Tables 1–3).

3.2.2. α and β Cells

In all mouse phenotypes fed the control Fe level (35 μg/g) the number of α and β cells/mean pancreatic islet area increased significantly between 12 and 24 months of age (Tables 4 and 5). Insulin and glucagon were not assayed due to lack of resources.

3.2.3. δ Cells

Among the control Fe groups, the number of δ cells/mean islet area increased significantly in the pseudoagouti and black mice between 12 and 24 months; however, it failed to do so in the yellow agouti or B6C3F$_1$ mice (Table 6). Somatostatin was not assayed due to lack of resources.

3.3. Fe overload

3.3.1. Iron scores and iron severity scores

After 24 months of 3500 or 5000 μg/g Fe consumption, the average iron score of pancreata of yellow agouti mice was more than twice as great as that of the pseudoagouti, black,

Table 1
Mean total islet area (mm^2)/pancreas after 12 and 24 months of Fe overload

	Control	Treated	Adjusted (Holm's) P[a]
Yellow agouti			
12 months	1815548 ± 428999 (11)	441105 ± 119892 (11)	0.006
P[b]	0.02	0.000	
24 months	3056281 ± 285555 (26)	1396980 ± 161883 (24)	0.000
Pseudoagouti			
12 months	333055 ± 72487 (12)	193709 ± 34433 (9)	ns
P	0.004	0.000	
24 months	695618 ± 88980 (21)	732533 ± 81505 (18)	ns
Black			
12 months	267533 ± 44180 (12)	298160 ± 58519 (12)	ns
P	0.000	0.001	
24 months	840698 ± 89220 (35)	634238 ± 63279 (27)	ns
$B6C3F_1$			
12 months	298279 ± 64756 (12)	122558 ± 36610 (12)	ns
P	0.000	0.000	
24 months	1279304 ± 1752 (31)	1077150 ± 99325 (32)	ns

[a] Adjusted $P_{\text{Control cf. Treated}}$.
[b] Unadjusted $P_{\text{12 months cf. 24 months}}$.

and $B6C3F_1$ mice (Table 8). The number of pancreas sections from yellow agouti mice containing Fe was more than twice that observed among the pseudoagouti, black, and $B6C3F_1$ mouse pancreata (Table 9).

The greater response of yellow agouti pancreatic islets and islet cells, as compared with the other pheno/genotypes, to iron overload is presumably associated with the greater absorption of Fe in this obese phenotype (Table 9).

3.3.2. α Cells

Treatment with the higher Fe doses resulted in decreased numbers of α cells/mean islet area only in the 12 months old yellow agouti and 24 months old $B6C3F_1$ mice (Table 4).

The number of α cells increased significantly between 12 and 24 months in the control and treated yellow agouti, pseudoagouti and $B6C3F_1$ mice but only among the control, and not in the treated, black mice (Table 4).

3.3.3. β Cells

Fe overload resulted in decreased numbers of β cells/mean islet area in all phenotypes, except in the 12 months old pseudoagouti and black mice and 24 months old $B6C3F_1$ mice (Table 5).

Significant increases in β cells between 12 and 24 months of age were observed in treated yellow agouti and $B6C3F_1$ mice, but not in the pseudoagouti or black mice (Table 5).

Table 2
Mean islet area (mm^2)/pancreas after 12 and 24 months of Fe overload

	Control	Treated	Adjusted (Holm's) P[a]
Yellow agouti			
12 months	36779 ± 5336 (11)	15936 ± 2943 (11)	0.001
P[b]	ns	ns	
24 months	41115 ± 3269 (26)	23338 ± 2495 (24)	0.000
Pseudoagouti			
12 months	10737 ± 1254 (12)	10560 ± 1133 (10)	ns
P	ns	0.02	
24 months	13860 ± 1162 (21)	15358 ± 1229 (18)	ns
Black			
12 months	10496 ± 1019 (12)	10345 ± 1045 (12)	ns
P	0.002	0.002	
24 months	15683 ± 800 (34)	16567 ± 1156 (27)	ns
$B6C3F_1$			
12 months	10308 ± 1269 (12)	9037 ± 1480 (12)	ns
P	0.000	0.000	
24 months	22884 ± 1752 (31)	20379 ± 1127 (32)	ns

[a] Adjusted $P_{\text{Control cf Treated}}$.
[b] Unadjusted $P_{\text{12 months cf. 24 months}}$.

Table 3
Mean number of islets/pancreas after 12 and 24 months of Fe overload

	Control	Treated	Adjusted (Holm's) P[a]
Yellow agouti			
12 months	43.3 ± 7.7 (11)	22.7 ± 3.9 (11)	0.04
P[b]	0.001	0.000	
24 months	74.0 ± 4.4 (26)	58.6 ± 4.7 (24)	0.03
Pseudoagouti			
12 months	29.8 ± 4.6 (12)	26.2 ± 6.0 (10)	ns
P	0.007	0.004	
24 months	47.6 ± 3.8 (21)	48.5 ± 4.0 (18)	ns
Black			
12 months	25.5 ± 3.1 (12)	27.2 ± 3.8 (12)	ns
P	0.000	ns	
24 months	49.3 ± 2.9 (35)	38.1 ± 3.2 (27)	0.01
$B6C3F_1$			
12 months	25.2 ± 3.8 (12)	11.3 ± 2.4 (12)	ns
P	0.000	0.000	
24 months	53.3 ± 3.3 (31)	52.6 ± 3.7 (31)	ns

[a] Adjusted $P_{\text{Control cf. Treated}}$.
[b] Unadjusted $P_{\text{12 months cf. 24 months}}$.

β cell concentration increased in all groups of control mice.

3.3.4. δ Cells

Fe overload significantly decreased the number of δ cells only in the 24 months old black mice and the 12 months old $B6C3F_1$ mice.

Among the treated mice, the numbers of δ cells increased in yellow agouti, pseudoagouti, and $B6C3F_1$, mice between 12 and 24 months of age, but failed to do so in the black mice (Table 6).

Among control groups, δ cell concentration increased with age only in pseudoagouti and black mice.

3.4. Liver

3.4.1. Iron scores and iron severity scores

After feeding 3500 or 5000 μg/g Fe for 12 months, histologic examination of liver sections, subjected to the Prussian Blue reaction, revealed the presence of intensely blue-stained Fe or hemosiderin in <25% of the hepatocytes in yellow agouti mice. While the amount of absorbed Fe was modest

Table 4
α Cells/mean islet area ± S.E. (N) after 12 and 24 months of Fe overload

	Control (μg/g)	Treated (μg/g)		P[a]
	35	3500	5000	
Yellow agouti				
12 months	19035 ± 2143 (10)		12274 ± 1856 (10)	0.03
P[b]	0.004		0.002	
24 months	28774 ± 1757 (26)		26718 ± 2268 (20)	ns
Pseudoagouti				
12 months	16848 ± 3365 (10)	12648 ± 3395 (10)		ns
P	<0.001	<0.001		
24 months	32843 ± 2388 (20)	31959 ± 2529 (18)		ns
Black				
12 months	12851 ± 2723 (11)		18665 ± 3780 (10)	ns
P	<0.001		ns	
24 months	26431 ± 1577 (34)		22418 ± 1707 (26)	ns
$B6C3F_1$				
12 months	13753 ± 2001 (12)		6127 ± 1514 (12)	0.006
P	0.001		<0.001	
24 months	21302 ± 1143 (30)		23323 ± 1373 (32)	ns

[a] Adjusted $P_{\text{Control cf. Treated}}$.
[b] Unadjusted $P_{\text{12 months cf. 24 months}}$.

Table 5
β Cells/mean islet area ± S.E. (*N*) after 12 and 24 months of Fe overload

	Control (μg/g)	Treated (μg/g)		P^a
	35	3500	5000	
Yellow agouti				
12 months	93786 ± 13352 (10)		42106 ± 6713 (10)	0.003
P^b	0.007		<0.001	
24 months	149856 ± 11048 (26)		107151 ± 9166 (20)	0.007
Pseudoagouti				
12 months	68534 ± 11006 (10)	48624 ± 10922 (10)		ns
P	0.02	ns		
24 months	98985 ± 7048 (20)	74382 ± 7898 (18)		0.02
Black				
12 months	52405 ± 9326 (11)		56075 ± 8363 (10)	ns
P	<0.001		ns	
24 months	106449 ± 6257 (34)		78678 ± 6014 (26)	0.003
$B6C3F_1$				
12 months	52031 ± 865 (12)		21596 ± 5084 (12)	0.007
P	0.001		<0.001	
24 months	99655 ± 8014 (30)		90418 ± 7002 (32)	ns

[a] Adjusted $P_{\text{Control cf. Treated}}$.
[b] Unadjusted $P_{\text{12 months cf. 24 months}}$.

with a diffuse distribution, there was extensive staining of the periportal and centrilobular areas. In contrast, pseudoagouti, black, and $B6C3F_1$ mouse livers exhibited blue staining in macrophages, Kupffer cells and 25–75% of the hepatocytes. This indicates that the rate of uptake of iron by the yellow agouti liver was lower than that of the lean pseudoagouti mouse livers as well as that of the other "lean" genotypes (Tables 8 and 9).

After feeding 3500 or 5000 μg/g Fe for 24 months, the Fe score of yellow agouti mice had increased to the same levels as the other pheno/genotypes, while the Fe scores of the latter had not changed from those observed after 12 months of Fe feeding. Fe staining was observed in macrophages, Kupffer cells, and 75–100% of the hepatocytes (Tables 8 and 9).

3.4.2. Hepatic tumors

3.4.2.1. Yellow agouti mice. Iron overload increased the prevalence of hepatocellular adenomas at 12 months from 18% to 45% among the obese yellow A^{vy}/a mice and may have had a somewhat inhibiting effect on hepatocellular carcinoma formation (Table 7).

Table 6
δ Cells/mean islet area ± S.E. (*N*) after 12 and 24 months of Fe overload

	Control (μg/g)	Treated (μg/g)		P^a
	35	3500	5000	
Yellow agouti				
12 months	7989 ± 1141 (10)		5143 ± 881 (10)	ns
P^b	ns		0.002	
24 months	10516 ± 619 (26)		10010 ± 874 (20)	ns
Pseudoagouti				
12 months	6301 ± 1105 (10)	6011 ± 1477 (10)		ns
P	<0.001	<0.001		
24 months	16090 ± 1159 (20)	17440 ± 1415 (18)		ns
Black				
12 months	4998 ± 722 (11)		6325 ± 979 (10)	ns
P	<0.001		ns	
24 months	10072 ± 638 (34)		7452 ± 567 (26)	0.004
$B6C3F_1$				
12 months	5672 ± 766 (12)		2773 ± 682 (12)	0.01
P	ns		<0.001	
24 months	7110 ± 550 (30)		8540 ± 660 (32)	ns

[a] Adjusted $P_{\text{Control cf. Treated}}$.
[b] Unadjusted $P_{\text{12 months cf. 24 months}}$.

Table 7
Hepatocellular tumor prevalence after 12 and 24 months of Fe overload

	Control (μg/g)	Treated (μg/g)	
	35	3500	5000
Yellow agouti			
12 months			
Adenomas	18% (2/11)		45% (5/11)
Carcinomas	9% (1/11)		(0/11)
Both	27% (3/11)		(0/11)
24 months			
Adenomas	54% (14/26)		58% (14/24)
Carcinomas	8% (2/26)		4% (1/24)
Both	19% (5/26)		33% (8/24)
Pseudoagouti			
12 months			
Adenomas	8% (1/12)	30% (3/10)	
Carcinomas	(0/12)	(0/12)	
Both	8% (1/12)	(0/12)	
24 months			
Adenomas	10% (2/21)	22% (4/18)	
Carcinomas	38% (8/21)	17% (3/18)	
Both	24% (5/21)	33% (6/18)	
Black			
12 months			
Adenomas	8% (1/12)		8% (1/12)
Carcinomas	(0/12)		(0/12)
Both	(0/12)		8% (1/12)
24 months			
Adenomas	23% (8/35)		15% (4/27)
Carcinomas	23% (8/35)		56% (15/27)
Both	26% (9/35)		(0/27)
$B6C3F_1$			
12 months			
Adenomas	8% (1/12)		(0/12)
Carcinomas	(0/12)		(0/12)
Both	(0/12)		(0/12)
24 months			
Adenomas	19% (6/31)		19% (6/32)
Carcinomas	6% (2/31)		6% (2/32)
Both	6% (2/31)		6% (2/32)

At 24 months of age adenoma prevalence among yellow agouti mice was similar in the control and Fe overload groups and considerably greater than at 12 months. Fe overload increased the prevalence of yellow agouti mice bearing both adenoma and carcinoma, but had no effect on the incidence of mice bearing only carcinoma (Table 7).

3.4.3. Pseudoagouti mice

At 12 months, lean pseudoagouti A^{vy}/a mice exhibited increased adenoma prevalence in the Fe overload group, but no carcinomas.

Among pseudoagouti mice fed Fe for 24 months, the prevalence of adenomas was essentially similar to that at 12 months; however, the prevalence of carcinoma was twice as great among the control as among the Fe overload group. There was also a considerable increase, similar to that observed among the yellow agouti mice, in the prevalence of mice bearing both an adenoma and a carcinoma in the control and Fe overload groups (Table 7).

3.4.4. Black mice

While almost no hepatocellular lesions were observed among the black mice fed Fe for 12 months, by 24 months the prevalence of adenomas and carcinomas had increased considerably. Fe overload doubled the prevalence of carcinomas compared to that observed among the control mice. Only in the control group were there any mice (26%) bearing both an adenoma and a carcinoma (Table 7).

3.4.5. $B6C3F_1$ mice

Among the $B6C3F_1$ mice fed Fe for 12 months, only one hepatocellular adenoma (and no carcinoma) was found in one control animal.

At 24 months the prevalence of adenomas was 19% in both control and Fe overload groups; the prevalence of carcinoma, as well as of adenoma + carcinoma, was 6% in control and treated mice (Table 7).

3.5. Heart

3.5.1. Iron scores and iron severity scores

Average iron scores of the yellow agouti mice were approximately twice as high as those of comparable pseudoagouti, black, and $B6C3F_1$ mice fed the diet containing 3500 or 5000 μg/g Fe for 24 months (Table 8). The iron severity scores for yellow agouti mice were also the highest among the four geno/phenotypes with more hearts exhibiting Fe-staining sections (Table 9).

4. Discussion

Ageing results from programmed developmental changes in the patterns of expression of genes regulating individual reactions in the metabolic and molecular pathways of the organism. The organismic manifestation of the phenotypic expression of the genome is designated the phenome. Age-associated changes in the phenome, in turn, alter the functional genomics (the phenotypic expression of each gene in the context of the whole genome) of the organism and are expressed as benign or malignant manifestations. Mutations induce these changes by altering the patterns of expression of other genes and by modulating interactions of molecular/metabolic processes and pathways.

4.1. Body weight

Yellow agouti mice gain excessive weight to about the age of 1.5 years, but then, as has been known for decades [5,13], begin to lose weight so that their body weight gradually declines to the “normal” level of non-yellow mice. Iron overload reduced this rate of weight loss (Fig. 3) and also markedly reduced the variability of food consumption (Fig. 4); however, whether interactions between iron, ectopic ASP and MC4R or other mechanisms are involved is unknown. In the present case, this “normal” weight level

Table 8
Average iron scores after 12 or 24 months of Fe overload

	35 μg/g		3500 μg/g		5000 μg/g	
	12 months	24 months	12 months	24 months	12 months	24 months
Pancreas						
Yellow agouti	0[a] (12)[b]	0 (40)	0 (12)	0.53 (36)	0 (12)	0.81 (32)
Pseudoagouti	0 (12)	0 (25)	0 (10)	0.19 (26)	–	–
Black	0 (12)	0 (40)	0 (11)	0.19 (42)	0 (11)	0.29 (42)
B6C3F$_1$ *A*/*a*	0 (12)	0 (46)	0 (11)	0.20 (45)	0 (12)	0.19 (43)
Liver						
Yellow agouti	0 (12)	0.12 (43)	1.42 (12)	2.59 (37)	1.92 (12)	3.09 (35)
Pseudoagouti	0.08 (12)	0.16 (25)	2.89 (9)	2.65 (26)	–	–
Black	0.08 (12)	0.12 (42)	3.00 (12)	2.86 (42)	3.00 (11)	3.43 (42)
B6C3F$_1$ *A*/*a*	0 (12)	0.38 (47)	2.83 (12)	2.91 (46)	2.92 (12)	2.89 (45)
Heart						
Yellow agouti	0 (11)	0.05 (43)	0.16 (12)	1.32 (38)	0 (11)	1.35 (34)
Pseudoagouti	0 (11)	0.04 (25)	0.22 (9)	0.46 (26)	–	–
Black	0 (12)	0.08 (40)	0 (11)	0.67 (42)	0 (11)	0.62 (39)
B6C3F$_1$ *A*/*a*	0 (9)	0.02 (47)	0 (11)	0.98 (45)	0 (12)	0.68 (44)

[a] Total iron scores of organs in dose group/number of organ sections examined.
[b] *N* = number of organ sections examined. One section per organ examined.

was reached about week 109 (Fig. 1). There may be background strain differences in age-related weight loss of yellow agouti mice since Kesterson (personal communication) has not observed it in obese lethal yellow A^y/a mice on a different strain background.

That this growth curve pattern is peculiar to yellow agouti mice and is not associated with "larger size mice" per se is indicated by the growth curve of B6C3F$_1$ hybrid mice that parallels that of the black *a*/*a* mice except for an increased rate of gain between weeks 6 and 14.

There is considerable anecdotal evidence that a small proportion of yellow agouti mice never become obese but retain normal body weight and are perfectly healthy and fertile. However, the only definitive studies to ascertain physiological and molecular differences between "heavier" and "lighter" yellow agouti mice appear to have been reported by us [45,46,48]. Mean body weights at 3–4 weeks and 9 months of age and liver and carcass (body weight − liver weight) weights at 9 months for "light" and "heavy" untreated control and phenobarbital-fed "light" and "heavy" groups of A^{vy}/A (C3H × VY)F$_1$ male mice [48] are shown in Table 10.

Even disregarding the effect of phenobarbital treatment, the final carcass weights of the initially "light" mice were significantly less than those of the initially "heavy" mice. Surprisingly, the percentage increases in body weights were quite similar between the light and heavy mice. This sug-

Table 9
Average iron severity scores after 12 or 24 months of Fe overload

	35 μg/g		3500 μg/g		5000 μg/g	
	12 months	24 months	12 months	24 months	12 months	24 months
Pancreas						
Yellow agouti	0[a] (0)[b]	0 (0)	0 (0)	1.6 (12)	0 (0)	1.2 (22)
Pseudoagouti	0 (0)	0 (0)	0 (0)	1.0 (5)	0 (0)	–
Black	0 (0)	0 (0)	0 (0)	1.3 (6)	0 (0)	1.3 (9)
B6C3F$_1$ *A*/*a*	0 (0)	0 (0)	0 (0)	1.0 (9)	0 (0)	1.0 (8)
Liver						
Yellow agouti	0 (0)	1.7 (3)	1.5 (11)	2.8 (34)	1.9 (12)	3.1 (35)
Pseudoagouti	1.0 (1)	2.0 (2)	2.9 (9)	2.8 (25)	–	–
Black	1.0 (1)	1.3 (4)	3.0 (12)	2.9 (41)	3.0 (11)	3.4 (42)
B6C3F$_1$ *A*/*a*	0 (0)	1.1 (16)	2.8 (12)	3.1 (44)	2.9 (12)	3.0 (43)
Heart						
Yellow agouti	0 (0)	1.0 (2)	2.0 (1)	1.9 (27)	0 (0)	1.5 (30)
Pseudoagouti	0 (0)	1.0 (1)	1.0 (2)	1.1 (11)	–	–
Black	0 (0)	1.5 (2)	0 (0)	1.2 (24)	0 (0)	1.3 (18)
B6C3F$_1$ *A*/*a*	0 (0)	1.0 (1)	0 (0)	1.5 (29)	0 (0)	1.4 (22)

[a] Total of iron scores of organs in dose group/number of Fe-containing organ sections.
[b] *N* = number of Fe-containing organ sections.

Table 10
Body, liver and carcass weights of "Heavy" and "Light" yellow agouti A^{vy}/A (C3H × VY)F_1 male mice at 3–4 weeks and 9 months of age

Age	Light control $\bar{x}$ g ± S.E. (*n*)	Heavy control $\bar{x}$ g ± S.E. (*n*)	Light PB-treated $\bar{x}$ g ± S.E. (*n*)	Heavy PB-treated $\bar{x}$ g ± S.E. (*n*)
Body weights				
3–4 weeks	25.6 ± 0.8 (6)	30.9 ± 1.7 (5)	27.9 ± 0.3 (6)	33.1 ± 0.9 (7)
9 months	43.2 ± 0.6	51.0 ± 0.7	43.0 ± 1.3	56.8 ± 0.8
% Increase	69	65	54	72
Liver weights				
9 months	1.55 ± 0.05	2.14 ± 0.1	2.41 ± 0.17	4.43 ± 0.26
Carcass weights[a]				
9 months	41.6 ± 0.6	48.9 ± 0.7	40.6 ± 1.1	52.4 ± 0.8

From Ref. [48].
[a] Body weight without liver weight.

gests that the differences in body weights were determined before weaning and indicates that a population of genetically identical A^{vy}/A (C3H × VY)F_1 male mice is composed of several physiologically/metabolically different subpopulations [49] with respect to pre-weaning rates of weight gain. These subpopulations also differ in various hepatic monooxygenase activities, in responsiveness of hepatic cytochrome P450 and monooxygenase activities to phenobarbital [48], as well as in susceptibility to hepatic adenoma formation [46].

According to Bray et al. [2], the level of desacetyl-α-MSH in the pituitary of A^{vy}/a mice is twice as high as in *a*/*a* mice. Treatment of A^{vy}/a mice with desacetyl-α-MSH induced a dose-related increase in muscle weight as well as increasing body weight to a greater degree than treatment with α-MSH [33]. In rats desacetyl-α-MSH treatment from postnatal day 0–1 to day 14 stimulated neonatal growth and also induced increased fat deposits [21]. If this is also true of mice, the pre-weaning differences in body weight between the "light" and "heavy" A^{vy}/a mice may be referable to possible differences in the hypothalamic levels of desacetyl-α-MSH since desacetyl-α-MSH is the predominant form produced by posttranslational processing in the murine hypothalamus [12].

This abnormal regulation of body weight of yellow agouti mice must be associated, directly or indirectly, with the presence of sufficiently high levels of ectopic ASP in the hypothalamus since the body weight curves of pseudoagouti A^{vy}/a mice, with very low levels of ectopic ASP, were essentially identical to those of black *a*/*a* siblings (Fig. 5).

4.2. Melanocortin-4 receptor

Food consumption is regulated, at least partly, by MC4R signaling in the hypothalamus. Binding of ectopic ASP to MC4R on hypothalamic neurons inhibits the receptor and results in a degree of hyperphagia leading to obesity. Ageing and iron overload (Fig. 4) appear to modulate the interaction of ectopic ASP with MC4R since food consumption of yellow agouti mice, after remaining relatively constant to about 50 weeks of age, begins to decrease until week 90 (Fig. 6). This is not true in the case of pseudoagouti A^{vy}/a or black *a*/*a* males (Fig. 6).

The isogenic pseudoagouti A^{vy}/a phenotype does not become obese but remains lean, suggesting that the very low concentration of ectopic ASP in these mice [6] may be insufficient to bind to a critical number of hypothalamic MC4R neurons. Nevertheless, ectopic ASP does influence, albeit to a low degree, some phenomic effects, such as carcass weight [47].

Body length of mice is increased in MC4R knock-out mice [16] as well as in yellow agouti A^y/a mice. Among same sex parabiosed A^y/a:A^y/a, A^y/a:*a*/*a*, and *a*/*a*:*a*/*a* Strain YS/ChWf mice, body length increase between 4/5 weeks of age and 28/31 weeks of age was greater ($P < 0.001$) in yellow agouti than in black mice. The increase in body length was also greater in mice joined to partners of the opposite genotype than in mice joined to partners of the same genotype [42].

If MC4R is expressed in a diversity of tissues in the mouse, as it is in the rat [26], ectopic ASP may inhibit MC4R signaling in these tissues and thus induce at least some of the aberrant aspects of the obese yellow agouti mouse phenome. For example, it seems reasonable to speculate that the increased long bone growth in yellow agouti mice [14] may be due to stimulation of osteoblast proliferation by ectopic ASP [27], whereas in MC4R knockout mice α-MSH may stimulate osteoblast proliferation [27], possibly by binding to MC5R.

4.3. Pancreas

The greater response of yellow agouti pancreatic islets and islet cells to iron overload, as compared with the other pheno/genotypes, is presumably associated with the greater absorption of Fe in this obese phenotype (Table 9).

Age-associated increases in pancreas size, islet number, and increased numbers of α, β, and δ cells per mean islet area were observed in all mouse phenotypes. In the yellow agouti mice this hyperplasia occurred, unexpectedly, in the presence

of continuing loss of body weight. In pre-weaning yellow agouti A^{vy}/a mice, β cell hyperplasia preceded hyperinsulinemia and obesity and subsequently accompanied them [37]. This supports the suggestion [17] that "hyperinsulinemia promotes adipogenesis and may initiate a cycle of increasing insulin resistance, compensatory hyperinsulinemia, and a progression to the diabetic state."

The age-associated islet cell hyperplasia observed here appears to be independent of body weight or food consumption since it also occurred in the lean isogenic pseudoagouti A^{vy}/a and congenic black a/a mice as well as in the B6C3F$_1$ mice. Pipeleers [28] has documented the existence of subpopulations of β cells that differ in glucose sensitivity. It remains to be ascertained whether the age-associated β cell hyperplasia documented here may be largely limited to subpopulations of low glucose sensitivity.

4.4. Cell proliferation

Unlike in non-yellow mice, human agouti protein (ASIP) is normally expressed in human adipose tissue, testis, heart, liver, kidney, ovary, and skin [19,41]. This implies that the protein has autocrine or paracrine functions in these organs and suggests that, in yellow agouti mice also, ectopic ASP may affect some cellular functions, e.g., proliferation, directly.

Smith et al. [34] found that, whereas α-MSH inhibits preadipocyte differentiation and adipocyte proliferation, transgenic ASP, specifically expressed in the murine fat pad, stimulates these processes. The presence of ectopic ASP also stimulates β cell proliferation in pancreatic islets of Langerhans [37], osteoblast proliferation [4], bladder epithelial hyperplasia [44], formation of hyperplastic alveolar nodules (HAN) in mammary glands [43] and formation of multiple hepatocellular adenomas [45]. Kuklin et al. [18] observed that the number of diethylnitrosamine-induced hepatocellular tumors in transgenic mice, in which ASP was synthesized only in the liver, was increased significantly in comparison with untreated control mice. This confirms our earlier observation [47] that ASP stimulated tumorigenesis even at the very low concentrations present in the livers of pseudoagouti A^{vy}/a female mice.

In accord with the characteristically earlier appearance of hyperplastic and neoplastic lesions in obese yellow agouti A^{vy}/a mice, both the control and Fe overload groups exhibited a greater prevalence of hepatocellular adenomas at 12 months of age than any other of the mouse phenotypes. In the earlier dose-finding study [40], increased hepatocyte proliferative activity in yellow agouti mice compared to black mice was indicated by proliferating cell nuclear antigen (PCNA) assays in liver of male mice fed 35 or 10,000 μg/g carbonyl iron for 90 days. As indicated in the following data reproduced here from that study with permission, iron overload also increased mitotic activity in both genotypes. It is important to note that the increased proliferative activity in A^{vy}/a livers was present at the control as well as at the high dose levels of iron.

	35 μg/g		10,000 μg/g	
	A^{vy}/a	a/a	A^{vy}/a	a/a
$G_1 + S + G_2 + M$	5.8 ± 0.8 ($P = 0.003$)	1.6 ± 0.8	15.8 ± 1.0 ($P < 0.001$)	6.7 ± 1.3
Total cells	2090 ± 15	2158 ± 26	2144 ± 19	2176 ± 21
Index	0.28 ± 0.04	0.07 ± 0.04	0.73 ± 0.05	0.31 ± 0.06

Among lean pseudoagouti A^{vy}/a mice, only the Fe overload group exhibited increased adenoma formation by 12 months of age. This suggests that the apparent promoting effect of Fe overload on adenoma formation among obese yellow agouti mice is real since analogous results were observed when lindane (γ-hexachloro-cyclohexane), instead of carbonyl Fe, was administered to yellow agouti and pseudoagouti mice [47]. The relatively low prevalence of hepatocellular carcinoma in yellow agouti mice [45,47] also supports previous suggestions [53] that ectopic ASP tends to stimulate hyperplastic, rather than neoplastic, transformation in different tissues. The greater prevalence of multiple hepatic adenomas observed in individual obese yellow (C3H × VY)F$_1$ male mice [45] was most likely a direct effect of the combined stimulation of hyperplasia by phenobarbital and ectopic ASP. An unresolved question is whether increased chromosomal fragility in yellow agouti mice (reviewed in [53]) may predispose these mice to hyperplasia and subsequently to neoplastic lesions.

4.5. Immunological aspects

Adult obese yellow agouti A^{vy}/a mice differ immunologically from the lean isogenic pseudoagouti A^{vy}/a and congenic black a/a mice by decreased antibody response to the T-cell dependent immunogen tetanus toxoid, enhanced antibody response to the T-cell-independent immunogen type III pneumococcal polysaccharide, decreased (unadjusted) rates of carbon clearance, and increased levels of serum IgA [30]. Possible relation of these immunological differences to the upregulation of the ubiquitous immunoglobulin transcription factor 2 (ITF2), a member of the tetraspannin gene family, by ASP and downregulation by α-MSH [9] is presently unknown. However, since ASP is continually transcribed in essentially all $A^{vy}/-$ tissues, it seems likely that some of its manifestations may be associated with its upregulation of *Itf2* in different tissues and consequent effects on various molecular/metabolic pathways (reviewed in [54]).

5. Summary and conclusion

Fe overload moderated the rate of body weight loss and ameliorated marked variability in the rate of decrease in food consumption beginning about 16 months of age in the yellow agouti A^{vy}/a mice. The possible role of MC4R signaling as affected by ASP binding and an unknown interaction with Fe remain to be investigated.

The rate of Fe uptake by yellow agouti livers was lower than that of isogenic pseudoagouti livers and the livers from the other non-obese mice. After 24 months of iron overload, however, the Fe score of the yellow agouti livers had increased to that of the other livers.

In contrast to the liver Fe uptake by the yellow agouti mice, the Fe uptake and severity scores of their hearts and pancreata were greater than in these organs of the non-obese mice.

In yellow agouti mice the number of pancreatic islets and total islet area were decreased after 12 and 24 months of Fe overload; however, this did not occur in the non-obese phenotypes.

The concentration of pancreatic α and β cells from all phenotypes treated with the control Fe dose increased between 12 and 24 months. Treatment with the higher Fe dose prevented such an increase in pseudoagouti and black mice.

Fe treatment increased the number of δ cells between 12 and 24 months in all phenotypes except the black mice.

Fe overload for 12 months increased prevalence of hepatocellular adenomas in yellow agouti and isogenic pseudoagouti mice. After 24 months of Fe overload adenoma prevalence in yellow agouti mice was greater than at 12 months and similar in the control and treated groups.

Among pseudoagouti mice fed the high Fe dose for 24 months carcinoma prevalence was 2× as great in the control as in the treated group.

Among the black mice, Fe overload doubled the number of carcinomas observed among the control mice.

While the hypothesis that these mice might serve as a tool for investigating hemochromatosis was not confirmed, the data did provide evidence of interactive effects of ASP, age, and carbonyl Fe in yellow agouti mice.

The present data demonstrate that the combination of yellow agouti A^{vy}/a, isogenic pseudoagouti A^{vy}/a, and congenic black a/a mice provide a practical animal model system for applying a dose–response systems biology approach to the investigation and understanding of the dysregulatory influence of ectopic ASP on the complex molecular-physiological matrix of the organism.

Acknowledgments

We thank Nadine Lowe, David Heard, and Donna Norton for performing the pancreas and islet cell morphometry measurements under the supervision of Alan Warbritton, Pathology Associates Inc., and Donald Hussen of Z-Tech Inc. for the statistical analyses. Helpful comments and suggestions by Donald B. Galbraith, Kathleen G. Mountjoy, and Randall L. Mynatt are much appreciated.

References

[1] Adan RA, Kas MJ. Inverse agonism gains weight. Trends Pharmacol Sci 2003;24:315–21.

[2] Bray GH, Shimizu H, Retzios AD, Shargill NS, York DA. Reduced acetylation of melanocyte stimulatory hormone (MSH): a biochemical explanation for the yellow obese mouse. In: Bjorntorp P, Rossner S, editors. Obesity in Europe 88. London: John Libbey & Co. Ltd.; 1989. p. 259–70.

[3] Bultman SJ, Michaud EJ, Woychik RP. Molecular characterization of the mouse agouti locus. Cell 1992;71:1195–204.

[4] Cornish J, Callon KE, Mountjoy KG, Bava U, Lin JM, Myers DE, et al. Alpha-melanocyte-stimulating hormone is a novel regulator of bone. Am J Physiol 2003;284:E1181–90.

[5] Dickie MM, Woolley GW. The age factor in weight of yellow mice. J Hered 1946;37:365–8.

[6] Duhl DMJ, Vrieling H, Miller KA, Wolff GL, Barsh GS. Neomorphic *agouti* mutations in obese yellow mice. Nat Genet 1994;8:59–65.

[7] Edwards CQ, Griffen LM, Goldgar D, Drummond C, Skolnick MH, Kushner JP. Prevalence of hemochromatosis among 11,065 presumably healthy blood donors. N Engl J Med 1988;318:1355–62.

[8] Frigeri LG, Wolff GL, Teguh C. Differential responses of yellow A^{vy}/A and agouti A/a (BALB/c × VY)F_1 hybrid mice to the same diets: glucose tolerance, weight gain, and adipocyte cellularity. Int J Obes 1988;12:305–20.

[9] Furumura M, Potterf SB, Toyofuku K, Matsunaga J, Muller J, Hearing VJ. Involvement of ITF2 in the transcriptional regulation of melanogenic genes. J Biol Chem 2000;276:28147–54.

[10] Galbraith DB, Wolff GL. Aberrant regulation of the agouti pigment pattern in the viable yellow mouse. J Hered 1974;65:137–40.

[11] Galbraith DB, Wolff GL, Brewer NL. Tissue microenvironment and the genetic control of hair pigment patterns in mice. Dev Genet 1979;1:167–79.

[12] Geis R, Martin R, Voigt KH. α-MSH-like peptides from the rat hypothalamus and pituitary: differences in the degree of N-acetylation. Horm Metab Res 1984;16:266–7.

[13] Goodrick CL. Body weight change over the life span and longevity for C57BL/6J mice and mutations which differ in maximal body weight. Gerontology 1977;23:405–13.

[14] Heston WE, Vlahakis G. Influence of the A^y gene on mammary gland tumors, hepatomas, and normal growth in mice. J Natl Cancer Inst 1961;27:1189–96.

[15] Holm S. A simple sequentially rejective multiple test procedure. Scand J Stat 1979;6:65–70.

[16] Huszar D, Lynch CA, Fairchild-Huntress V, Dunmore JH, Fang Q, Berkemeier LR, et al. Targeted disruption of the melanocortin-4 receptor results in obesity in mice. Cell 1997;88:131–41.

[17] Kieffer TJ, Habener JF. The adipoinsular axis: effects of leptin on pancreatic β-cells. Am J Physiol Endocrinol Metab 2000;278:E1–14.

[18] Kuklin AI, Mynatt RL, Klebig ML, Kiefer LL, Wilkison WO, Woychik RP, et al. Liver-specific expression of the agouti gene in transgenic mice promotes liver carcinogenesis in the absence of obesity and diabetes. Mol Cancer 2004;3. Art.17.

[19] Kwon HY, Bultman SJ, Löffler C, Chen W-J, Furdon PJ, Powell JG, et al. Molecular structure and chromosomal mapping of the human homolog of the agouti gene. Proc Natl Acad Sci USA 1994;91:9760–4.

[20] Luna LG. Perl's method for iron. In: Manual of histologic staining methods of the Armed Forces Institute of Pathology. 3rd ed. New York: McGraw Hill; 1968. pp. 184–185.

[21] Mauri A, Melis MR, Deiana P, Loviselli A, Volpe A, Argiolas A. Melanocortins and opioids modulate early postnatal growth in rats. Regul Pept 1995;59:59–66.

[22] Michaud EJ, van Vugt MJ, Bultman S, Sweet HO, Davisson MT, Woychik RP. Differential expression of a new dominant agouti allele (A^{iapy}) is correlated with methylation state and is influenced by parental lineage. Genes Dev 1994;8:1463–72.

[23] Miller MW, Duhl DMJ, Vrieling H, Cordes SP, Ollmann MM, Winkes BM, et al. Cloning of the mouse *agouti* gene predicts a

secreted protein ubiquitously expressed in mice carrying the *lethal yellow* mutation. Genes Dev 1993;7:454–67.
[24] Mintz B, Bradle M. Mosaic expression of a tyrosinase fusion gene in albino mice yields a heritable striped coat color pattern in transgenic homozygotes. Proc Natl Acad Sci USA 1991;88:9643–7.
[25] Mountjoy KG, Robbins LS, Mortrud MT, Cone RD. The cloning of a family of genes that encode the melanocortin receptors. Science 1992;257:543–6.
[26] Mountjoy KG, Wu CSJ, Dumont LM, Wild JM. Melanocortin-4 receptor messenger ribonucleic acid expression in rat cardiorespiratory, musculoskeletal, and integumentary systems. Endocrinology 2003;144:5488–96.
[27] Mountjoy, K.G., Dumont, L.M., Wu, C.-S. J., Callon, K.E., Cornish, J. Osteoblast cells: model system for studying interactions between melanocortin receptors and their ligands. ENDO 2004 [Abstract P2-27].
[28] Pipeleers DG. Heterogeneity in pancreatic β-cell population. Diabetes 1992;41:777–81.
[29] Reeves PG, Nielsen FH, Fahey Jr GC. AIN-93 purified diets for laboratory rodents: final report of the American Institute of Nutrition ad hoc writing committee on the reformulation of the AIN-76A rodent diet. J Nutr 1993;123:1939–51.
[30] Roberts DW, Wolff GL, Campbell WL. Differential effects of the mottled yellow and pseudoagouti phenotypes on immunocompetence in A^{vy}/a mice. Proc Natl Acad Sci USA 1984;81:2152–6.
[31] Satterthwaite FW. An approximate distribution of estimates of variance components. Biometrics Bull 1946;2:110–4.
[32] Shapiro SS, Wilk MB. An analysis of variance test for normality (complete samples). Biometrika 1965;52:591–611.
[33] Shimizu H, Shargill NS, Bray GA, Yen TT, Gesellchen PD. Effects of MSH on food intake, body weight and coat color of the yellow obese mouse. Life Sci 1989;45:543–52.
[34] Smith SR, Gawronska-Kozak B, Janderova L, Nguyen T, Murrell A, Stephens JM, et al. Agouti expression in human adipose tissue. Functional consequences and increased expression in Type 2 diabetes. Diabetes 2003;52:2914–22.
[35] Steel RGD, Torrie JH. Principles and procedures of statistics. 2nd ed. New York: McGraw-Hill Book Company; 1980. pp. 401–437.
[36] Thompson SW, Hunt RD. Microscopic histochemical methods for the demonstration of minerals. In: Selected histochemical and histopathological methods. Springfield, IL: Charles C. Thomas Publishers; 1966. p. 576–614.
[37] Warbritton A, Gill AM, Yen TT, Bucci T, Wolff GL. Pancreatic islet cells in preobese yellow $A^{vy}/-$ mice: relation to adult hyperinsulinemia and obesity. Proc Soc Exptl Biol Med 1994;206:145–51.
[38] Whittaker P, Skikne BS, Covell AM, Flowers C, Cooke A, Lynch SR, et al. Duodenal iron proteins in idiopathic hemochromatosis. J Clin Invest 1989;83:261–7.
[39] Whittaker P, Wamer W, Calvert RJ. Effect of chronic iron overload on iron status, lipid peroxidation, cell proliferation, and DNA damage. J Trace Elem Exp Med 1992;5:227–36.
[40] Whittaker P, Dunkel VC, Bucci TJ, Kusewitt DF, Thurman JD, Warbritton A, et al. Genome-linked toxic responses to dietary iron overload. Tox Path 1997;25:556–64.
[41] Wilson BD, Ollmann MM, Kang L, Stoffel M, Bell GI, Barsh GS. Structure and function of *ASP*, the human homolog of the mouse *agouti* gene. Hum Mol Genet 1995;4:223–30.
[42] Wolff GL. Growth of inbred yellow (A^y/a) and non-yellow (a/a) mice in parabiosis. Genetics 1963;48:1041–58.
[43] Wolff GL, Medina D, Umholtz RL. Manifestation of hyperplastic alveolar nodules and mammary tumors in "viable yellow" and non-yellow mice. J Natl Cancer Inst 1979;63:781–5.
[44] Wolff GL, Gaylor DW, Frith CH, Suber RL. Controlled genetic variation in a subchronic toxicity assay: susceptibility to induction of bladder hyperplasia in mice by 2-acetylaminofluorene. J Toxicol Env Health 1983;12:255–65.
[45] Wolff GL, Morrissey RL, Chen JJ. Amplified response to phenobarbital promotion of hepatotumorigenesis in obese yellow A^{vy}/A (C3H × VY) F-1 hybrid mice. Carcinogenesis 1986;7:1895–8.
[46] Wolff GL, Morrissey RL, Chen JJ. Susceptible and resistant subgroups in genetically identical populations: response of mouse liver neoplasia and body weight to phenobarbital. Carcinogenesis 1986;7:1935–7.
[47] Wolff GL, Roberts DW, Morrissey RL, Greenman DL, Allen RR, Campbell WL, et al. Tumorigenic responses to lindane in mice: potentiation by a dominant mutation. Carcinogenesis 1987;8:1889–97.
[48] Wolff GL, Leakey JEA, Bazare JJ, Harmon JR, Webb PJ, Law MG. Susceptibility to phenobarbital promotion of hepatotumorigenesis: correlation with differential expression and induction of hepatic drug metabolizing enzymes in heavy and light male (C3H × VY) F_1 hybrid mice. Carcinogenesis 1991;12:911–5.
[49] Wolff GL. Variability in gene expression and tumor formation within genetically homogeneous animal populations in bioassays. Fund Appl Toxicol 1996;29:176–84.
[50] Wolff GL. Obesity as a pleiotropic effect of gene action. J Nutr 1997;127:1897S–901S.
[51] Wolff GL, Kodell RL, Moore SJ, Cooney CA. Maternal epigenetics and methyl supplements affect agouti gene expression in A^{vy}/a mice. FASEB J 1998;12:949–57.
[52] Wolff GL, Kodell RL, Kaput JA, Visek WJ. Caloric restriction abolishes enhanced metabolic efficiency induced by ectopic agouti protein in yellow mice. Proc Soc Exptl Biol Med 1999;221:99–104.
[53] Wolff GL, Roberts DW, Mountjoy KG. Physiological consequences of ectopic agouti gene expression: the yellow obese mouse syndrome. Physiol Genomics 1999;1:151–63.
[54] Wolff GL. Regulation of yellow pigment formation in mice: a historical perspective. Pigment Cell Res 2003;16:2–15.
[55] Yen TT, Allan JA, Yu P, Acton MA, Pearson DV. Triacylglycerol contents and in vivo lipogenesis of *ob*/*ob*, *db*/*db* and A^{vy}/a mice. Biochim Biophys Acta 1976;441:213–20.